JOURNAL OF STRUCTURAL BIOLOGY **115,** 186–198 (1995)

# A Discourse on Modeling F-Actin

CLARENCE E. SCHUTT, MICHAEL D. ROZYCKI, AND JAMES C. MYSLIK

*Department of Chemistry, Henry H. Hoyt Laboratory, Princeton University, Princeton, New Jersey 08544*

AND

U. LINDBERG

*Department of Zoological Cell Biology, WGI, Arrhenius Laboratories for Natural Sciences, Stockholm University, S-10691 Stockholm, Sweden*

Received March 27, 1995

## INTRODUCTION

A major challenge for structural biologists is to obtain atomic resolution models for higher order structures. In favorable instances, the intact particle can be crystallized and all atomic positions and bonds within the macromolecular complex can be determined to the resolution limit of the data. Icosahedrally symmetric virus particles exemplify the application of crystallography to structures of polymeric complexes at sufficient resolution to visualize the amino acid side-chain interactions stabilizing intermolecular interfaces (Harrison *et al.,* 1978). Tobacco mosaic virus is an outstanding example of the successful phasing of a high-resolution fiber X-ray diffraction pattern by multiple isomorphous replacement (Namba and Stubbs, 1986). But, what can be done when crystals of the intact structures cannot be obtained or when the existing fiber patterns simply do not extend to high enough resolution?

## COLLISION ON THE AUFBAUBAHN

Several years ago we argued that, in the special case in which components of higher order structures could be crystallized with accessory proteins that prevent polymerization, information about bonds which stabilize higher order structures might be found in crystal contacts between monomeric subunits (Schutt, 1987). We called this path to knowledge the *Aufbaubahn* to signify the process of building up atomic models of complex biological structures from the crystal structures of their constituents. Recently, great strides have been made toward an atomic-level description of the force-generating couple in muscle contraction with the determination of the structures of muscle actin ($\alpha$-actin) (Kabsch *et al.,* 1990; McLaughlin *et al.,* 1993) and myosin subfragment 1 (Rayment *et al.,* 1993a). This work led to a class of models for F-actin using low-resolution X-ray fiber diffraction data as the primary constraint for docking the actin monomer into the filament helix (Holmes *et al.,* 1990; Lorenz *et al.,* 1993; Tirion *et al.,* 1995) and to a model for the complex of F-actin and myosin S1 (Rayment *et al.,* 1993b; Schröder *et al.,* 1993). On the other hand, the structure of nonmuscle actin ($\beta$-actin) complexed with profilin (Schutt *et al.,* 1989, 1993), with its organization of actin molecules into "ribbons" with extensive actin–actin interfaces (Fig. 1), suggested that a filament model could be arrived at in a different way, using observed crystal contacts (Schutt *et al.,* 1993). As it happens, the actin–actin bonds observed in profilin–actin crystals cannot be reconciled with those occurring in the docked model of the Heidelberg group, and so one or the other modeling approach must lead to the wrong answer (Schutt *et al.,* 1995). While freely acknowledging the merits and attractiveness of the "docking" method, we are surprised that the "crystal contact" approach is dismissed by some investigators without their full understanding of the arguments involved.

We appreciate the opportunity to explain how our model-building conclusions are at variance with those of the Heidelberg group. Our purpose here is not to persuade the reader to accept a new model of F-actin per se, since we have not yet presented a *bona fide* model of our own. Rather, we hope to convey our arguments for the validity of the "crystal contact" rationale. We feel that this is an important argument to understand, since crystallographers often utilize crystal contacts to infer *in vivo* intermo-



1047-8477/95 $12.00

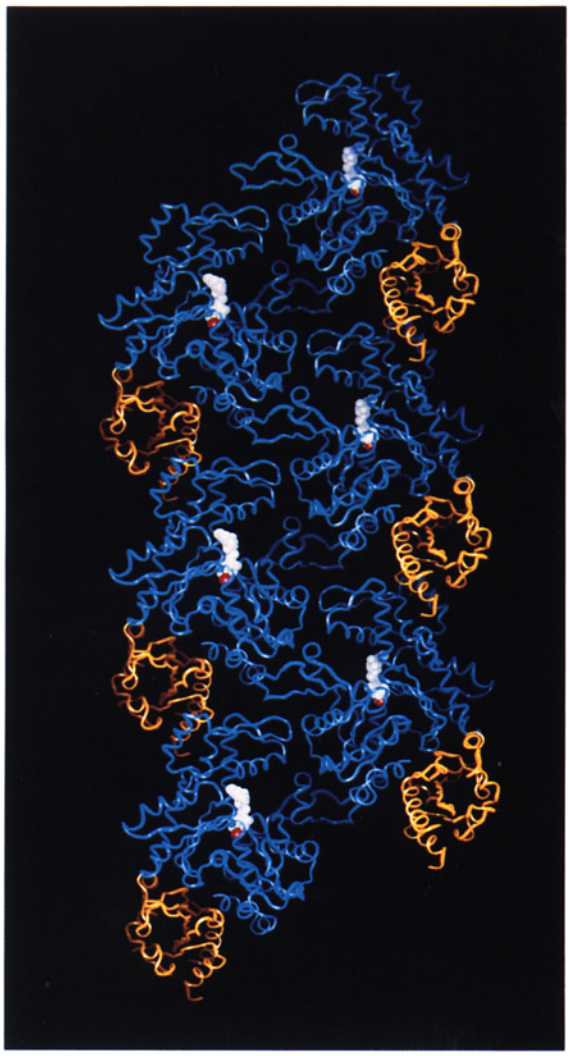

**FIG. 1.** The profilin–actin ribbon. Actin molecules (blue) are arranged about a vertical $2_1$-screw axis. Profilin molecules (gold) insert between actin molecules on each side of the screw axis. Each actin monomer contains one bound ATP molecule (white). The actin–actin "ribbon contact" lies at the interface between each pair of actin molecules lying across the screw axis. The solvent-accessible surface buried between two actin monomers is 1770 Å$^2$, calculated according to Lee and Richards (1971) with X-PLOR (Brünger, 1992) using a probe radius of 1.4 Å. The value given here differs somewhat from that given in Schutt *et al.* (1993) due to subsequent refinement of the structure reported therein.

lecular bonds (for example, Story *et al.,* 1992; Brown *et al.,* 1993; Cho *et al.,* 1994; Shapiro *et al.,* 1995). If a reliable atomic model of F-actin has in fact been achieved by coupling molecular docking with X-ray fiber diffraction at medium resolution (Holmes, 1994), an important precedent will have been set in structural biology, and the falsification of the ribbon-to-helix conjecture would provide a warning to structural biologists attempting other arguments on the basis of observed crystal contacts.

## WHAT ARE REASONABLE MODELING EXPECTATIONS FROM AVAILABLE DATA?

The actin filament has not been crystallized. Thus, the certainty provided by a structure based on tens of thousands of phased reflections, such as was the case for viruses, is not present. However, the helically symmetric actin filament is an instance in which the availability of atomic coordinates of the monomer and medium resolution, X-ray fiber diffraction data offer the opportunity of modeling the higher order structure (Holmes, 1994). By fixing the diameter of the model filament and making only the assumption that the actin monomer does not change conformation in the initial transfer from the DNase I:$\alpha$-actin crystal complex to the helically symmetric F-actin filament, Holmes *et al.* (1990) found a unique monomer orientation by minimizing the R-factor, which compares observed and calculated structure amplitudes. The question then arises of how much confidence can be placed in a model obtained from medium resolution fiber data.

Our analysis starts with the observation that no structural model can be called a "known" structure, even when an "almost perfect fit" to diffraction data is claimed. This fundamental premise is rooted in the crystallographic problem of "homometric sets," namely, that there is no unique solution to the Patterson function (Blundell and Johnson, 1976). Since an enormous number of structural models can fit a diffraction pattern to any desired accuracy, all models must be considered trial structures. The success of crystallography rests on the consistency of proposed structures with the "rules of the game," the cumulative set of bond lengths and bond angles that has amassed over the years from a combination of all sources, including spectroscopy and theoretical calculations (Brändén and Jones, 1990). Crystal structures reported at even 3 Å resolution with good refinement statistics are occasionally found which later prove to have substantial chain tracing errors when higher resolution is reached. Final acceptance of a model comes down to having the number of independent observations exceed by a substantial margin the number of parameters required to define it, as is customary in any application of numerical analysis.

In crystallographic refinement, the number of observed structure factors typically exceeds the number of parameters to be determined (positional coordinates, temperature factors, etc.) by a factor of 10 (Blundell and Johnson, 1976). Additional overdetermination is provided by constraining bond lengths and angles to standard values (Engh and Huber, 1991). Protein structures must have dihedral angles for the peptide backbone that fall within allowed regions of Ramachandran space. Crystallographers

report instances of "strained" peptide bonds and offer explanations for them that become themselves part of the trial model. Whether a structure is considered acceptable or not depends, in part, on the plausibility of these auxiliary arguments. Correspondingly, any model that contains atomic resolution detail carries with it a set of auxiliary assumptions that were invoked to reduce the number of structural parameters below the number of independent observations. An example of such an assumption might be that a subdomain is largely unchanged in going from the crystal structure to its position in the higher order structure.

The need to understand and evaluate the source of auxiliary assumptions is especially acute when an atomic resolution model is to be docked into a supramolecular structure, since the molecule is likely to change its conformation as it is incorporated into the higher order structure. This is the lesson provided by the icosahedral virus structures, one of the few classes of biological polymers resolved at atomic resolution. Not only are hinge angles between subdomains of the monomers observed to vary in accommodating the different packing environments in the capsid, but the amino and carboxy termini are seen adopting radically different structures in intact particles (Harrison *et al.,* 1978). Thus, any attempt to model an oligomeric structure from a crystal structure of the monomer must start with the expectation that the monomer conformation will change; the amino and carboxy termini in particular should be scrutinized for the possibility of lengthy excursions that might provide additional stabilizing interactions, as should other regions of the molecule whose structures lend themselves to conformation reorganization. Importantly, however any *ad hoc* adjustments to, or accumulations of, strain in the structure made during the process of modeling must be justified by plausible energetic arguments. Since these adjustments become part of the supramolecular model, they must be tested independently of it as discrete auxiliary arguments.

An example of such an auxiliary argument is the "hydrophobic plug" hypothesis of F-actin. A drawback to the initial placement of actin monomers in the "docked" model was that there did not appear to be extensive enough intermolecular contacts between the two strands of the filament to explain how they could remain associated (Holmes *et al.,* 1990). This was remedied by rebuilding a loop consisting of residues 264–273, which appeared to be in an energetically unfavorable conformation in the DNase I:$\alpha$-actin crystals, into a $\beta$-hairpin "plug" which fit into a hydrophobic pocket formed by two adjacent actin subunits on the opposite strand of the filament. This was a reasonable approach, since, for the reasons given above, it was to be expected that certain regions of the actin monomer would change on being incorporated into the helical lattice of the filament. However, a warning flag was raised when the residues in question were compared in the crystal structures of $\alpha$-actin and $\beta$-actin (Schutt *et al.,* 1993). Although these residues have the same polypeptide backbone conformation, the side-chain rotomer conformations of two and only two residues (Glu 259 and Phe 223) are drastically different. Specifically, the positions of these side chains are interchanged in the two structures (Fig. 2a). While these side chains do indeed lie in an energetically unfavorable conformation in $\alpha$-actin, with the charged carboxylate of Glu 259 lying next to the aromatic ring of Phe 266, their positions in $\beta$-actin are actually stabilizing, since Glu 259 is able to form a salt bridge with Arg 312, and Phe 223 is now lying near the ring of Phe 266. In addition, reforming residues 264–272 into a plug would require overcoming the energy barrier of breaking at least two main-chain hydrogen bonds (Fig. 2b). Thus, assuming that $\alpha$-actin and $\beta$-actin use similar chemistry in forming intermonomeric bonds within the filament, the crystallographic data do not support an *ad hoc* remodeling of this loop into a projecting plug. Indeed, this appears to be in accord with the most recent variation on the Heidelberg model, arrived at by a normal mode analysis of the conformation of the actin monomer in the filament model, in which the residues comprising the putative "plug" show no tendency to adopt the projecting conformation proposed originally (Tirion *et al.,* 1995). In summary, the "hydrophobic plug" argument used an *ad hoc* change to a high-resolution structural feature (formation of secondary structure, a $\beta$-hairpin) in order to rescue a model from an unsatisfactory low-resolution feature (weak monomer contacts). Because of its plausibility, the change was assimilated into the entire filament model without rigorous testing. This is an important example to bear in mind when evaluating the origins of claims of "atomic" resolution for structural models of higher order structures.

Docking an atomic-resolution monomer structure into a filament model using fiber diffraction data cannot give a truly atomic-resolution model if the fiber data do not extend to a resolution level comparable to that used in solving the monomer structure (DeRosier, 1990). Furthermore, subsequent refinements of such models should be held to the same rigors of atomic-resolution model building as the original crystal structures. A case in point is the directed mutation algorithm refinement (Lorenz *et al.,* 1993) of the docked model of the actin filament, in which the monomer structure within the filament was allowed to vary in conformation about the initial model. Although the refined model was judged to give a "nearly perfect" fit to fiber diffraction data at

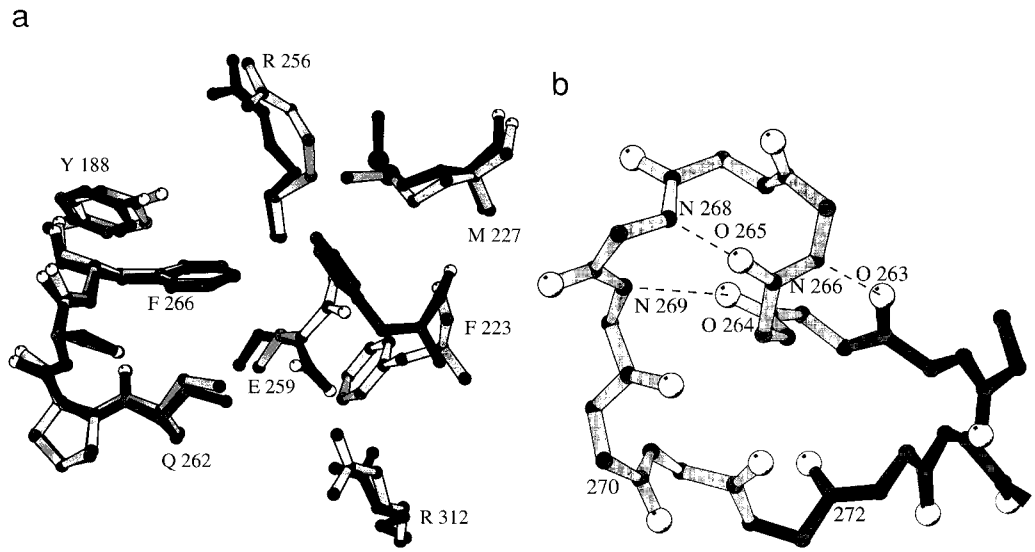


**FIG. 2.** Local environment of residues in the loop connecting subdomains 3 and 4 of actin. Atom colors are white (O), gray (C), and black (N, S) and atomic radii are drawn at 0.9 Å for O, C, and N and at 1.5 Å for S. (a) Interchange of side-chain positions of F223 and E259. Models of α-actin (Kabsch *et al.,* 1990) and β-actin (Schutt *et al.,* 1993) were aligned in subdomain 3 as described in Fig. 2 of Schutt *et al.* (1993). Atom connections are white for α-actin and gray for β-actin. The conformational change between the two isoforms allows E259 in β-actin to form an electrostatic interaction with R312, while F223 of β-actin forms a closer hydrophobic interaction with F266, one of the residues postulated to form a "hydrophobic plug" within the actin filament (Holmes *et al.,* 1990). For simplicity, main-chain atoms are not shown for Y188, R256, and R312, and side-chain atoms $C^{\delta}$, $N^{\epsilon}$, and $O^{\epsilon}$ are not shown for Q262. (b) Conformation of main-chain atoms of residues 262–272 of β-actin. Atom connections are white for residues that need to change conformations to form the "hydrophobic plug" (Holmes *et al.,* 1990). Hydrogen bonds are likely between O263 and N266 (3.12 Å), between O265 and N268 (2.67 Å), and between O264 and N269 (2.97 Å). Figure made using MOLSCRIPT (Kraulis, 1991). Residue abbreviations: Y, tyrosine; F, phenylalanine; M, methionine; R, arginine; E, glutamate; Q, glutamine.

0.8 nm, it is difficult to accept this claim, since there was no discussion of whether refinement-induced structural changes in the actin monomer were obtained at the expense of bond geometry or fit to allowed Ramachandran space. The quality of the refined monomer structure should be demonstrably equivalent to the starting crystal structure, or else the refinement method has no validity. Indeed, the recent normal mode refinement of the filament, which does address the quality of the final monomer structure, makes more modest claims (13.0 vs 5.5% R-factor) of the goodness of fit to the diffraction data (Tirion *et al.,* 1995).

Lee Makowski has examined the general question of how many independent structural parameters can be determined from modeling two-dimensional diffraction data, and discussed the factors influencing the quality of the data and the reliability of parameters that can be obtained (Makowski, 1991). He provides a rule of thumb, based on the Shannon assumption that independent intensity estimates are spaced at intervals of $\frac{1}{2}d$ along each layer line, for estimating the number of independent variables that can be determined from fiber diffraction data. Using the known diameter and axial repeat of the actin filament (9.5 and 2.75 nm, respectively), Makowski's formula suggests that 15 structural parameters can be determined from diffraction data at the 1.66-nm deconvolution limit which was used to orient the actin monomer in the actin helix (Holmes *et al.,* 1990). This means that, in principle, if the actin monomer were to be represented by four spheres corresponding to the individual subdomains, the configuration of these subdomain spheres could just barely be determined, assuming that the number of determinable parameters is somewhat overestimated (Makowski, 1991). At 0.8 nm resolution, which is beyond the deconvolution limit of the fiber data (Holmes *et al.,* 1990), the number of determinable independent parameters is roughly 108. This corresponds to about 35 residues, less than 10% of those occurring in the actin monomer. Clearly, the fiber data is underdetermined to give a truly atomic resolution refinement of F-actin. Thus, refinement strategies such as the directed mutation algorithm (Lorenz *et al.,* 1993) should be viewed skeptically, since the number of variables refined was much larger than allowed by the resolution limit of the fiber data, even though the number refined in any one step was kept small. In effect, at the point at which the high-resolution crystal structure of the monomer is changed by subdomain and side-chain movements during the refinement process, all knowledge of atomic-level detail is lost, and interresidue contacts that result from such refinements become hypothetical.

## MODEL FITTING TO MOLECULAR ENVELOPES

A number of investigators have attempted to corroborate the Heidelberg docking model of F-actin (Holmes *et al.,* 1990; Lorenz *et al.,* 1993; Tirion *et al.,* 1995) using electron microscopy and image reconstruction techniques (Milligan *et al.,* 1990; Bremer *et al.,* 1991, 1994; Orlova and Egelman, 1992, 1993; Owen and DeRosier, 1993; Mendelson and Morris, 1994; Schmid *et al.,* 1994). While differing more or less in specific details, these studies unanimously claim consistency or agreement with the docked model. In some cases, claims are even made that specific molecular detail is discernible in such images, such as the "hydrophobic plug" (Bremer *et al.,* 1994) or conformational changes in subdomain 2 (Orlova and Egelman, 1993). Conversely, one attempt has been made to dismiss the profilin–actin ribbon for having biological relevance on the basis of a claimed "poor fit" to electron micrograph reconstructions of F-actin (Egelman, 1994). Even though in this instance the "poor fit" was due to the mistaken use of the ribbon as a *bona fide* filament model, instead of simply as the starting point for model building (Schutt *et al.,* 1994), the general question can be raised of how low-resolution electron microscopy should be used to confirm or dismiss atomic models of supramolecular structures.

Reconstructions from electron micrographs of F-actin generally contain information to a limiting resolution of between 2.5 and 1.3 nm, depending on the sample type and preservation conditions. Using Makowski's formula (Makowski, 1991), one would expect between 6 and 39 independent determinable parameters to be available from data at this resolution, although this number may be doubled because of the additional phase information. Because this amount of information is not sufficient to build a structural model *ab initio,* microscopists rely on previously built atomic models which are "smoothed" to the resolution of their data to assess fits of structures to reconstructed images. For example, Bremer and colleagues demonstrate that there is density in the actin filament in the region matched to the rebuilt loop consisting of residues 264–273 on actin (Bremer *et al.,* 1994), despite the fact that the resolution of their electron density maps would not permit them to follow the polypeptide fold of these residues *ab initio.* This does not mean, however, that the hydrophobic plug hypothesis has been proven by electron microscopy, since other filament models may very well account for this bridging density. All that can be inferred is that, unless these residues are in the plug conformation, the docked model is not consistent with their reconstructions. Thus, what was originally introduced into the model as an *ad hoc* adjustment has become an essential underpinning of the model, at least if the reconstructions of Bremer *et al.* are to be fit. It remains to be seen how well these reconstructions match the newest normal mode refinement of the docked model, which does not have the hydrophobic plug (Tirion *et al.,* 1995). Meanwhile, since the hydrophobic "plug" is an ineliminable feature of the docked model, because to give it up is tantamount to accepting a "notch" where electron micrograph images show density (Bremer *et al.,* 1994), is it fair to dismiss this model from further consideration because the plug is not substantiated by crystallographic observation, as described above? Probably not, although such "asymmetry" in the willingness to accept or reject a model on the basis of such a small piece of density is perhaps an indication of the need for "double blind"-type controls on interpretations of electron micrograph reconstructions (Pollard *et al.,* 1993).

For many observers, the natural concern is whether a given model "looks like" electron micrograph reconstructions of F-actin, and so it is important to address two questions: what are the origins of the electron density envelopes that constitute reconstructed images and how does one objectively assess the goodness of fit of a model to real data? As discussed above, crystallographers interpret molecular models through a number of constraints and assumptions which become part of the final model. One such constraint is the atomic temperature factor (or B-factor), which is a measure of the mobility or disorder in a region of the model. The crystal structures of actin show that subdomains 2 and 4 are particularly susceptible to disorder, depending on how actin interacts with neighboring molecules in crystals. Subdomain 2 has relatively low disorder (judged from local B-factors) when it forms a complex with DNase I (Kabsch *et al.,* 1990), whereas complexed to actin in profilin–activity crystals it is somewhat more disordered (higher B-factors) (Schutt *et al.,* 1993), and in the absence of complexed protein it is so disordered as to be indecipherable in electron density maps (McLaughlin *et al.,* 1993). Subdomain 4, on the other hand, is quite disordered in DNase I–actin and gelsolin segment 1–actin crystals, to the point where part of it (residues 200–207) had to be left unbuilt in one structure (McLaughlin *et al.,* 1993), but it is much better ordered in profilin–actin crystals (Schutt *et al.,* 1993). Thus, a serious concern for a microscopist fitting a model of actin to electron micrograph reconstructions must be whether the electron density envelope is a reliable representation of a molecular boundary, or whether it might be attenuated by variations of molecular mobility or disorder in the same way as high-resolution maps in X-ray crystallography. In short, one cannot necessarily expect an overly good fit of any model of F-actin to electron micrograph recon-

structions because, based on actin crystallography, it is probably unrealistic to assume perfectly isotropic electron density envelopes. This argument is germane, because the main difference between the orientation of actin monomers in the Heidelberg docked model and in the profilin–actin ribbon involves approximately an interchange of the positions of subdomains 2 and 4 and another interchange of the positions of subdomains 1 and 3. Subdomains 1 and 3 are of almost identical size and average atomic temperature factor, while subdomains 2 and 4 differ significantly in both properties. Indeed, subdomain 2 is difficult to fit to electron micrograph reconstructions in some investigations (Milligan *et al.,* 1990; Bremer *et al.,* 1991; Orlova and Egelman, 1992; Mendelson and Morris, 1994), while subdomain 4 is observed to "spill out" of electron density envelopes in reconstructions of the actin–scruin complex (Schmid *et al.,* 1994). These observations could arise from local attenuation of electron density in either of these domains, but they could just as easily result from switching subdomains 2 and 4 if the incorrect monomer orientation has in fact been chosen. Until such questions are dealt with experimentally, it appears premature to interpret shifts of electron density, especially in stained specimens, in such specific structural terms as subdomain rotations (Orlova and Egelman, 1993).

## CORROBORATION OF THE HEIDELBERG MODEL BY OTHER MEANS

It is clear that the docking approach taken by the Heidelberg group and the crystal-contact approach advanced by us will never give models for the actin filament at a resolution exceeding that of data obtained from fibers themselves. What can we expect, then, in terms of our ability to understand the chemistry of the actin filament? The ongoing changes to the intermonomeric filament contacts and actin subunit structure in different refinements of the docked model (Holmes *et al.,* 1990; Lorenz *et al.,* 1993; Tirion *et al.,* 1995) demonstrate that the idea of obtaining a unique, "atomic" model of F-actin has already been abandoned. Until methods are developed to extract atomic resolution data from F-actin, the best that can be achieved is an ever-increasing degree of confidence in an *approximate* model based on its ability to predict the outcome of various experiments that depend on the relative positions of various chemical groupings in the model. Examples of such corroborative tests are chemical crosslinking, functional assays with mutated residues, identification of labeled residues by electron microscopy, fluorescence energy transfer, and other spectroscopic measures of distance and position. *Approximate* models thus obtained would indeed be useful in identifying features such as the general location of docking sites for actin binding proteins, but they can never be useful in describing the function of actin and its associated proteins in high-resolution chemical terms.

The docked filament model of the Heidelberg group has the correct diameter and helical parameters for the actin filament (Holmes *et al.,* 1990). Although this in itself is not corroborating evidence for the model, since the helical parameters were assumed constraints in the model-building process, it is an important criterion for the plausibility of the docking technique that the actin monomer structure could satisfy these constraints without undue clashing between adjacent subunits. In addition, the model appears to account for the known polarity of the actin filament. The angled attachment of myosin heads defines "pointed" and "barbed" ends of the filament (Huxley, 1963), which have been used to classify actin-binding proteins as having a "barbed end" or a "pointed end" capping function (Pollard and Cooper, 1986). DNase I is known to bind to the pointed end, whereas gelsolin binds to the barbed end. The crystal structure of gelsolin segment 1 bound to actin (McLaughlin *et al.,* 1993) reveals that gelsolin binds to a surface that is on the opposite end of the Heidelberg model from where DNase I would bind. The successful placement of the binding sites for these proteins at ends of the actin filament (and not, for example, along the sides of the filament) is important corroborating evidence for the Heidelberg model, although, of course, other models that also would place the actin-binding surfaces of DNase I and gelsolin at filament ends are equally corroborated.

A second line of corroborating evidence for the Heidelberg model is provided by electron microscope images of filaments labeled with a monomaleimido undecagold adduct at Cys 374, the penultimate residue of the actin sequence. The radial position of Cys 374 inferred from this experiment agrees within reasonable error bounds with the expectations of the Heidelberg model (Milligan *et al.,* 1990), even though, strictly speaking, the original filament model was based on a monomer structure from crystals in which the carboxy-terminal residues had been proteolytically removed from actin (Kabsch *et al.,* 1990). When structures of actin complexed with gelsolin segment 1 and profilin were obtained that had intact carboxy termini, it was clear that the sulfhydryl of Cys 374 was buried in a relatively solvent-inaccessible, hydrophobic pocket (McLaughlin *et al.,* 1993; Schutt *et al.,* 1993), indicating that reagents specific for this residue, including the gold label, must disrupt the local $\alpha$-helical structure at the carboxy terminus of actin, or that the monomer changes conformation in this region during polymerization.

Other corroborating evidence exists for the docked

model, not the least of which is its positioning of the amino terminus of actin so as to be accessible to actin-binding proteins such as myosin S1 (Holmes *et al.,* 1990; Rayment *et al.,* 1993b). It is not within our scope to critically review all of the data. However, it is instructive to discuss certain types of data which are inadequately controlled to be truly definitive, but which, nevertheless, have become part of the "canon" of data adduced to support the Heidelberg model. The "hydrophobic plug," while perhaps losing structural significance in the latest filament refinement (Tirion *et al.,* 1995), provides a good example of this kind of data.

Site-directed mutagenesis has been used (Chen *et al.,* 1993) to create a mutant yeast (*S. cerevisiae*) actin with the residue change $L_{267}D$ (using a residue numbering scheme based on homology to α-actin; the mutant is denoted $L_{266}D$ in the original paper), which lies in the putative plug region. Haploid cells with this mutation had a wild-type phenotype at and above 20°C, but showed moderate cold sensitivity at 4°C. Since hydrophobic interactions are destabilized at low temperatures, this result was interpreted (Chen *et al.,* 1993; Lorenz *et al.,* 1993) as being consistent with a disruption of plug-mediated hydrophobic interactions within the filament as predicted (Holmes *et al.,* 1990). However, the crystal structure of β-actin provides a much different interpretation. In the β-actin monomer, the side chain of Leu 267 lies in a very hydrophobic pocket consisting of side chains from Leu 180, Tyr 188 (aromatic ring), Ala 260, Pro 264 (ring), and Met 269, as well as the $C^{\beta}$ methylene group of Asp 184. These residues are identical in sequence in yeast actin, except that residue 269 is a leucyl. Assuming that yeast actin has a similar structure to β-actin in this region, the Leu-to-Asp mutation then puts a negatively charged residue in the middle of a hydrophobic pocket, as well as adjacent to a preexisting negative charge on Asp 184. This would be expected to destabilize the native conformation of this region, especially at low temperatures where any remaining hydrophobic interactions between the methylene group on Asp 267 and the surrounding residues would be diminished. This is the likely cause of the 15°C decrease in the melting temperature of mutant actin relative to the wild type (Chen *et al.,* 1993). Thus, the temperature sensitivity of the Leu-to-Asp mutant could be explained simply in terms of hydrophobic forces that maintain the *native conformation* of the monomer, rather than a plug-mediated bridge between filament strands.

In another example, Amberg and co-workers explain a disruption of actin–actin contacts in a yeast two-hybrid system in terms of mutations in the receiving pocket of the "plug" (Amberg *et al.,* 1995). The yeast two-hybrid system works by fusing one ancillary protein to the GAL4 DNA-binding domain and another to the GAL4 activation domain (Amberg *et al.,* 1995). If the two ancillary proteins bind to each other, they bring the GAL4 domains together to form a complete functional protein, allowing growth on a medium containing aminotriazine. Implicit in this experiment is the unsubstantiated assumption that the dimer formed from the two ancillary proteins is physiologically important. Actin forms at least two structurally distinct dimers (Millonig *et al.,* 1988). For the hydrophobic plug to play a role in stabilizing an actin dimer in the two-hybrid experiment, the dimer formed would have to be one that preserved the one-start helical ($N \rightarrow N + 1$) actin:actin contact. There is no way of verifying this from the type of data obtained in two-hybrid experiments. In fact, since the plug works in the context of a three-body interaction, fitting into a pocket formed by the junction of the $N + 1$ and $N - 1$ molecules (Holmes *et al.,* 1990), it seems overly optimistic to expect such an interaction to be preserved in the two-hybrid dimerization, especially when the stability of the dimer is claimed to be sensitive to individual residue substitutions (Amberg *et al.,* 1995).

The above examples demonstrate the importance of withholding judgment on the significance of mutagenesis results until a thorough understanding of the structural consequences of residue changes is available; the testing of models of intermolecular interactions is much more difficult than testing intramolecular models where mutagenesis has been successful (Baase *et al.,* 1992). A last example shows that other types of biochemical information also require thorough evaluation before being cited as corroborating evidence for a particular model. Gln 41 and Lys 113 of F-actin can be crosslinked by *N*-(4-azidobenzoyl)-putrescine (ABP), constraining

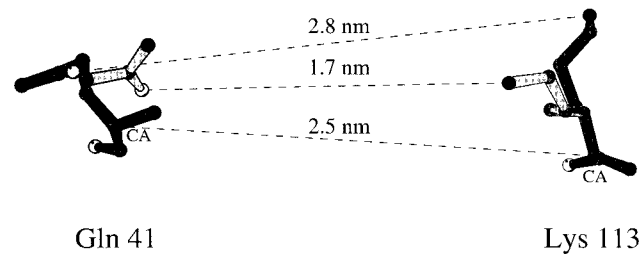


**FIG. 3.** Relative positions of Gln 41 of monomer N and Lys 113 of monomer $N + 2$ within the model of F-actin (Holmes *et al.,* 1990) refined by normal mode analysis (Tirion *et al.,* 1995). Atoms are colored white (O), gray (C), and black (N) and are scaled at atomic radii of 0.9 Å. Interatomic distances are shown between $C^{\alpha}$ atoms (CA) and between $O^{\epsilon}$ of Gln 41 and $N^{\epsilon}$ of Lys 113 in both the native conformation (gray atom connections) and with rotomers allowing closest possible approach between reactive atoms (white atom connections). Distance between $C^{\alpha}$ atoms differs slightly from that reported by Tirion *et al.* (1995). Figure made using MOLSCRIPT (Kraulis, 1991).

$O^{\epsilon}$ of Gln 41 to lie within 1.1 nm of $N^{\epsilon}$ of Lys 113 (Hegyi *et al.,* 1992). This would allow a *maximum* distance between $C^{\alpha}$ atoms of 2.2 nm. Tirion *et al.* (1995) argue that the inter-$C^{\alpha}$ distance between these residues (2.4 nm between the N and N + 2 monomers) in the normal mode refinement is consistent with the crosslinking data. However, such inter-$C^{\alpha}$ spacing does not guarantee consistency. Figure 3 shows that the distance from Gln 41 $O^{\epsilon}$ to Lys 113 $N^{\epsilon}$ of the neighboring (N + 2) monomer in the Tirion refinement of the Heidelberg model is 2.8 nm, which is actually greater than the inter-$C^{\alpha}$ distance. This happens because the sidechains of these residues point *away* from each other rather than *toward* each other in their refined conformations in the filament. Rotating the side chains to their closest possible approaches brings the two residues only to within 1.7 nm, still 6 Å too far away to accommodate the crosslinker within the filament.

In the profilin–actin ribbon, Gln 41 and Lys 113 are separated by 4.1 nm, and, because Lys 113 is on the "outside" of the ribbon, there is no way to move these residues close enough in a ribbon-based filament model to accommodate the distance requirements on an intrafilament crosslinker. Does this mean that neither model can be correct since they are both, strictly speaking, incompatible with the results of Hegyi and co-workers? Of course not. The Heidelberg model would become consistent with the crosslinking data if main-chain conformational changes in either the N or N + 2 monomers in the filament allowed a reorientation of the residues in question. On the other hand, a ribbon-based filament model would also be consistent with the same data if the crosslinking occurred between, rather than within, filaments. Pairing of actin filaments assembled *in vitro* is quite common (e.g., see Fig. 7 in Millonig *et al.,* 1987), and solutions of ABP-labeled F-actin are birefringent (Hegyi *et al.,* 1992), indicating that significant interfilament alignment and bundling takes place.

## CRYSTAL CONTACTS AS A BASIS FOR MODELING F-ACTIN

Structural analysis of crystalline bovine profilin–β-actin (Schutt *et al.,* 1989, 1993) and bovine profilin in actin-free crystals (Cedergren-Zeppezauer *et al.,* 1994) provides an alternative basis for constructing an actin filament model (Schutt *et al.,* 1993, 1995; Rozycki *et al.,* 1994). This argument rests on the premise that the oligomeric form of actin discerned in profilin–actin crystals, termed by us the "ribbon," can be transformed into the classical helical form of actin seen in electron micrographs. Thus, a claim is being made not only for the significance of actin–actin ribbon contacts in crystals, but for the biological relevance of the ribbon-to-helix transition itself. It is for these reasons that we have adduced arguments for the possible role of ribbon-to-helix transitions in muscle contraction (Schutt and Lindberg, 1992, 1993) and in profilin-regulated assembly of F-actin (Schutt *et al.,* 1993; Cedergren-Zeppezauer *et al.,* 1994). However, it should be apparent that proposing the basis for a new model and actually producing the detailed structural and energetic pathway between ribbon and helix are two different matters, a distinction that cannot be ignored in view of the ever-present risk of overinterpreting the available low-resolution diffraction data.

What is an actin ribbon? As observed in profilin–actin crystals (Fig. 1), each actin monomer is related to its neighbors along the *b*-axis by a rotation of 180° and a translation of 3.56 nm. The intermolecular contacts between monomers related by this screw operation are extensive (1770 $Å^2$) and chemically and sterically complementary, displaying the characteristics of genuine oligomeric structures (Schutt *et al.,* 1993). The diameter of the ribbon is 9.5 nm (Schutt *et al.,* 1989). One end of the ribbon corresponds to the DNase I-binding surface, while the opposite end presents the gelsolin-binding surface, thereby establishing that the polarity of the ribbon is the same as that of F-actin into which it is presumed to transform. The radial position of Cys 374 is 2.16 nm, consistent with the gold-labeling data (Milligan *et al.,* 1990) and fluorescence resonance energy transfer measurements (Moens *et al.,* 1994). (Initially, the position of Cys 374 was incorrectly assigned to a radial position of 3.3 nm, under the assumption that sulfhydryl-directed, heavy atom compounds reacted with this residue (Schutt *et al.,* 1989). We now know that these compounds react instead with another cysteine in β-actin, Cys 272 (Rozycki *et al.,* 1995).) These structural characteristics would be expected if the ribbon were truly related to F-actin by an untwist of 13° and a stretch of 0.83 nm per monomer. Thus, a ribbon-based model of F-actin appears to be corroborated by the same structural evidence as the Heidelberg docked model, although this corroboration should be considered preliminary until a *bona fide* model is derived from the ribbon structure.

One criticism of the profilin–actin ribbon as a biologically important structure is that it does not place the amino terminus of actin on the outermost edge of the filament (Egelman, 1994). This is an important criticism, because electron micrograph reconstructions of F-actin bound to myosin S1 (Rayment *et al.,* 1993b; Schröder *et al.,* 1993) as well as Fab fragments directed against the amino terminus of actin (Orlova *et al.,* 1994) are both claimed to localize the amino terminus of actin in the position

predicted by the Heidelberg docked model. A point to consider is that the amino terminus of actin, while not on the outermost edge of the ribbon (nor in a ribbon-derived filament model), is still in a solvent-accessible region that could interact with an incoming Fab fragment (Fig. 4). Reconstructed images of Fab-decorated F-actin lack over 90% of the electron density expected for the mass of the fragment, probably because of mobility at the N-terminus of actin (Orlova *et al.,* 1994), and there is no way of knowing what portion of the Fab is actually visible. In fact, this is a good example of the difficulty cited above of fitting electron density envelopes obtained by electron microscopy to molecular models without knowing to what extent the envelope is attenuated by disorder and mobility. Since it is not known where the Fab–F-actin interface lies in the reconstruction, it is not possible to identify the density shown in the reconstructions with the precise position of the amino terminus of actin (Schutt *et al.,* 1994).

A piece of data cited as strongly corroborating the docking model of myosin S1 and F-actin (Rayment *et al.,* 1993b; Schröder *et al.,* 1993) is that the amino terminus of actin can be crosslinked to myosin S1 in a region (Tyr 626–Gln 647) that is enriched in glycines and lysines (Sutoh, 1982). It is claimed from docking these two proteins that the crosslinked residues in myosin would lie on top of the amino terminus of actin, but this is not known for certain, since the 626–647 stretch of residues is absent from the crystal structure of myosin S1, owing to disorder (Rayment *et al.,* 1993a). In fact, it is not even known what range of conformations this stretch of 20 residues could actually adopt in the docked model and what the energetic tradeoffs would be. A complication is that, at least under nucleotide-free conditions, Fab fragments and myosin S1 heads can apparently bind to the amino terminus of actin simultaneously (DasGupta and Reisler, 1992). This is difficult to reconcile with the current docking of F-actin and myosin S1 (Rayment *et al.,* 1993b), in which the steric blocking of the amino terminus of actin by myosin would seem to preclude the simultaneous binding of a large antibody fragment. Thus, it seems more likely that the 626–647 region of myosin binds at a site adjacent to, but not actually covering, the amino terminus of actin. This could be achieved by a positioning of the amino terminus of

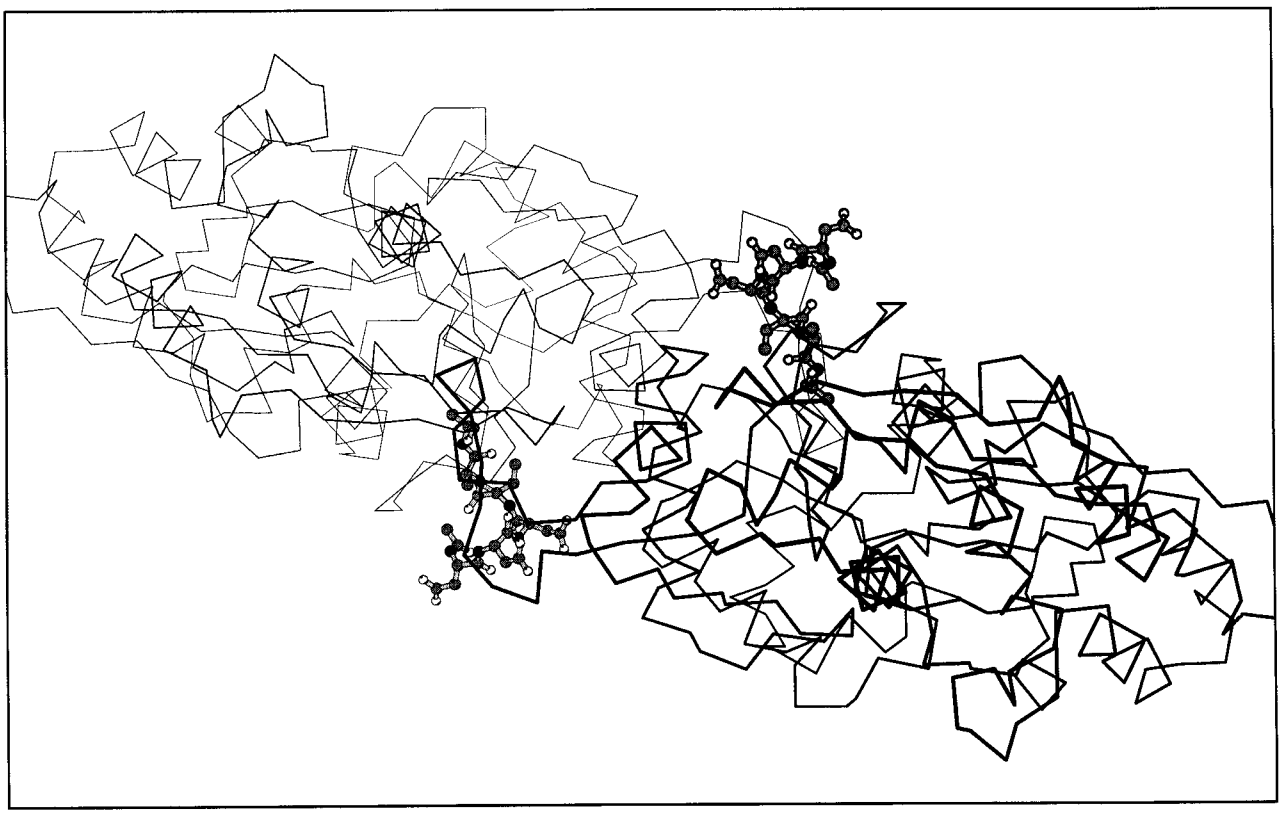

**FIG. 4.** Position of the amino terminus of β-actin in the profilin–actin ribbon. Two actin monomers are shown (thin and thick $C^{\alpha}$ trace, respectively) looking along the ribbon axis in the -b direction, e.g., from the "pointed end" of the ribbon (monomer at right). Amino-terminal residues, including the *N*-acetyl moiety, are shown in ball-and-stick motif (O, white; C, gray; N, black). Figure made using MOLSCRIPT (Kraulis, 1991).

actin away from the center of mass of S1, accompanied perhaps by an extension of the 626–647 loop toward it. It is easy to envision such an arrangement in the profilin–actin ribbon (Fig. 4), but this is speculative in the absence of a *bona fide* filament model.

### OTHER EVIDENCE FOR THE SIGNIFICANCE OF CRYSTAL CONTACTS

Aside from these structural characteristics, there is corroborating evidence from other sources that the ribbon is an oligomeric state of actin related to F-actin. Many of these arguments are described elsewhere (Schutt *et al.,* 1995). There is one major chemical difference between the actin ribbon and classical F-actin. The bound nucleotide in the ribbon is ATP (Schutt *et al.,* 1993), whereas in the helical form it is ADP (Korn *et al.,* 1987). Thus, it is presumed that during the ribbon-to-helix transition, one molecule of inorganic phosphate is released per monomer, suggesting that relatively large free energy changes can be made available to perform biological work. This is the basis for our theory of muscle contraction (Schutt and Lindberg, 1992, 1993; Schutt *et al.,* 1995).

It is well known that ATP hydrolysis accompanies the G-to-F transition under *in vitro* conditions in such a way that hydrolysis occurs at some point after addition of actin monomers to growing filaments (Korn *et al.,* 1987). This leads to ATP "caps" at the barbed ends of growing filaments (Carlier *et al.,* 1984). Experimental evidence suggests that significant conformational changes in the actin monomer occur during this polymerization process (Oosawa, 1977). Furthermore, the barbed and pointed ends of actively elongating filaments are different in their affinities for both actin (Korn *et al.,* 1987 and references therein) and profilin–actin (Pring *et al.,* 1992; Pantaloni and Carlier, 1993). Remarkably, overexpression of profilin in Chinese hamster ovary cells, which from mass action arguments would seem to favor depolymerization, leads to an apparent stabilization of filamentous structures in living cells (Finkel *et al.,* 1994).

Our analysis of protein–protein interfaces in crystalline profilin–actin suggests how these facts might be tied together by the occurrence of ribbon-to-helix transitions in freshly added actin monomers at filament barbed ends (Cedergren-Zeppezauer *et al.,* 1994). The central idea is that an actin–ATP–profilin complex has a higher affinity for the barbed end because the previously added complexes constitute a different binding surface from that seen at the pointed end. Not only are the actin monomers at the two ends different in conformation and state of bound nucleotide, but the barbed end presents a bound profilin to the pointed end of the incoming complex (Fig. 5). This structural role for profilin was not anticipated prior to the crystallographic work, but its contribution to the binding energy is significant, based on buried surface area (1100 Å$^2$) and surface complementarity. In this profilin-guided polymerization reaction, part or all of the Gibbs free

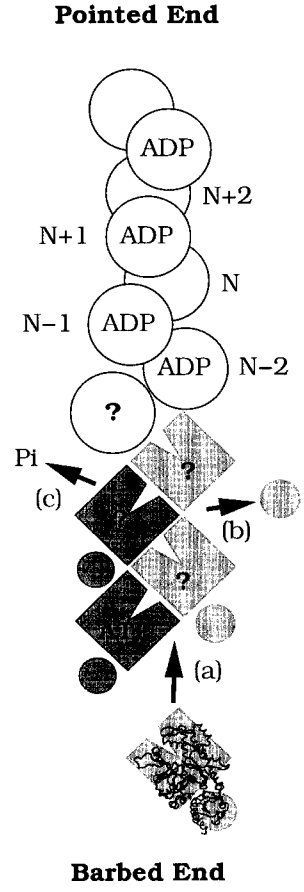


**FIG. 5.** Possible structural role of profilin–actin ribbon segments in capping actin filaments. As proposed (Pantaloni and Carlier, 1993), profilin (circle) could play an active role in F-actin assembly by adding actin molecules (notched squares) to filament barbed ends (step a). The ribbon contact would be related to the 1-start helical contact ($N-1 \rightarrow N$ and $N \rightarrow N+1$) in the filament, while profilin would block the formation of the 2-start helical contact ($N-2 \rightarrow N$ and $N \rightarrow N+2$). Hydrolysis of ATP to ADP and subsequent dissociation of $P_i$ accompany, but are not tightly linked to, addition of actin monomers to growing filaments (Carlier and Pantaloni, 1986; Korn *et al.,* 1987). In the model shown, structural changes in actin, probably linked to ATP hydrolysis (Pantaloni and Carlier, 1993), lead to subsequent dissociation of both profilin (step b) and $P_i$ (step c) from actin monomers as they undergo a twist of 13° and a lattice spacing contraction of 0.83 nm to form the helical lattice. Step b could take place prior to, along with, or sometime after step c. Question marks denote monomers whose nucleotide content is uncertain but may contain either ATP or ADP and undissociated $P_i$ (the ADP–$P_i$ state (Carlier and Pantaloni, 1986)). The relative size of the ribbon segment and its coincidence with ATP-, ADP-$P_i$, and ADP-containing monomers is shown for illustrative purposes only and should not be interpreted as a strict prediction. For comparison, it appears that the GTP cap on microtubule protofilaments may be as small as one tubulin dimer (Drechsel and Kirschner, 1994).

energy released during the ribbon-to-helix transition could be used to catalyze the dislodgement of profilin from actin. However, the formation of an additional actin–actin contact (the two-start helical contact) from the two surfaces previously bound to profilin would restore this free energy, suggesting the capacity for actin filaments to perform biological work. In the absence of profilin, actin filament assembly may or may not proceed through the same ribbon–helix transition depicted in Fig. 5. This model for *self-assembling in-line motors* has obvious implications for understanding cell motility.

This model makes the prediction that growing filaments, at least in the presence of profilin, have barbed end caps which contain either ATP or ADP and undissociated $P_i$ (Carlier and Pantaloni, 1986) and which are structurally distinct from the ADP-containing interior of the filament lattice. In particular, these caps would be twisted by up to 13° and stretched by 0.83 nm per monomer. Although nucleotide-linked changes in actin filaments have been implicated by electron microscopy (Orlova and Egelman, 1992; Lepault *et al.,* 1994), such specific changes in the filament lattice have yet to be observed. However, the profilin–ATP–actin cap is probably a transient state, an assembly intermediate. As such, the ribbon form of actin is similar in concept to the transition state in an enzymatic reaction, important for understanding kinetics but difficult to observe directly. Therefore, it probably would not be present in solution in amounts detectable by spectroscopic or equilibrium binding methods, since any signal reporting this interaction would have strength proportional to the number of growing filaments rather than to the concentration of profilin:actin. The fact that the ribbon is a *high-energy* transition state relative to the classical F-actin helix is also the probable explanation for the failure of electron microscopists to observe it.

In this light, recent studies of the dependence of microtubule structure on nucleotide hydrolysis are very interesting. Microtubules are analogous to actin filaments in that hydrolysis of GTP to GDP on tubulin dimers lags behind addition of GTP dimers to growing tubules (Carlier *et al.,* 1987). This leads to GTP "caps" at growing ends of microtubules which control their assembly and disassembly through dynamic instability (Mitchison and Kirschner, 1984). It has been shown that sheared ends of microtubules exhibit a splaying of individual protofilaments at the ends of microtubules (Mandelkow *et al.,* 1991; see also Fig. 5 of Drechsel and Kirschner, 1994). This splaying is not observed in images of normal growing filaments and was interpreted by Mandelkow *et al.* as an effect arising from the removal of the GTP-dimer cap. Exposure of the underlying GDP-dimer "body" leads to rapid microtubular disassembly in the dynamic instability model (Mitchison and Kirschner, 1984), and it seems likely that this disassembly is rooted in the structural changes captured by cryopreservation (Mandelkow *et al.,* 1991). This means that the GDP-dimer body of a microtubule is in a high-energy state that is prevented from unraveling by the presence of the GTP cap, which appears to be as small as a single GTP dimer at the end of each protofilament (Drechsel and Kirschner, 1994). Thus, GTP-dimer caps on normal microtubules are probably too small to be discerned by electron or X-ray diffraction techniques. However, electron imaging and analysis of microtubules assembled with the nonhydrolyzable GTP analogue guanylyl-($\alpha,\beta$)-methylene-diphosphonate (GMPCPP) have made it possible to examine the structural differences between the microtubule GDP lattice and a GTP-like lattice. Relative to the GDP lattice, the GTP-like lattice is stiffer, has less protofilament twist, and has a 1.5-Å-longer dimer repeat distance along the protofilament (Vale *et al.,* 1994; Hyman *et al.,* 1995). Thus, there is significant evidence that nucleotide hydrolysis plays an important role in structural transitions during microtubule growth. Observation of such structural changes in F-actin, involving ribbon-helix transitions, will require similar success at trapping states that normally exist only transiently and at small, localized regions at filament ends.

Ironically, the difficulty of directly observing the ribbon outside of the context of profilin:actin crystals is reminiscent of the failure of microscopists to obtain unambiguous evidence for the "rotation" of myosin heads required by most cross-bridge theories of muscle contraction (Pollard *et al.,* 1993). The standard response is that X-ray diffraction of contracting muscle fibers reveals large changes in intensity along the myosin-based layer lines, indexing on 42.9 nm, as tension develops from the relaxed state (Huxley, 1973). However, the actin ribbon can also account, in principle, for part of this change, since the ribbon is commensurate with the myosin lattice ($12 \times 3.57$ nm = 42.9 nm). Thus, as we have argued elsewhere (Schutt and Lindberg, 1992; Schutt *et al.,* 1995), myosin-induced helix-to-ribbon transitions, followed by force-producing ribbon-to-helix contractions, form a plausible basis for explaining muscle contraction, including the muscle fiber diffraction data.

## CONCLUSION

Our purpose has been to lay bare the structure of the controversy surrounding the two approaches to arriving at a structural model for F-actin. The criticism of data used to support the Heidelberg model (Holmes *et al.,* 1990) should not be equated with rejection of the model itself. The Heidelberg model could yet turn out to be the best representation of

the structure of F-actin once controlled experiments have rigorously ruled out other classes of models. Indeed, the reason that we have been cautious in presenting a *bona fide* model of F-actin of our own is out of recognition of just how difficult the problem is and the latitude of possible models allowed by available constraints. The biology of the profilin–actin interaction implies that more radical conformational changes in actin are needed than those assumed in the Heidelberg model to explain the behavior of these remarkable molecules. Crystallographic information from polymorphic profilin–actin crystals may be the key to understanding the nature of such changes (Rozycki *et al.,* 1995; Schutt *et al.,* 1995).

We thank Michael Lorenz and Monique Tirion for providing coordinates for their F-actin models. This work was supported by grants from the National Institutes of Health, the Swedish Cancer Foundation, the Swedish Natural Science Research Council, and the Granholms Foundation.

## REFERENCES

Amberg, D. C., Basart, E., and Botstein, D. (1995) Defining protein interactions with yeast actin in vivo, *Nature Struct. Biol.* **2,** 28–34.

Baase, W. A., Eriksson, A. E., Zhang, X.-J., Heinz, D. W., Sauer, U., Blaber, M., Baldwin, E. P., Wozniak, J. A., and Matthews, B. W. (1992) Dissection of protein structure and folding by directed mutagenesis, *Faraday Discuss.* **93,** 47–65.

Blundell, T. L., and Johnson, L. N. (1976) Protein Crystallography, Academic Press, San Diego.

Brändén, C.-I., and Jones, T. A. (1990) Between objectivity and subjectivity, *Nature* **343,** 687–688.

Bremer, A., Henn, C., Goldie, K. N., Engel, A., Smith, P. R., and Aebi, U. (1994) Towards atomic interpretation of F-actin filament three-dimensional reconstructions, *J. Mol. Biol.* **742,** 683–700.

Bremer, A., Millonig, R. C., Sutterlin, R., Engel, A., Pollard, T. D., and Aebi, U. (1991) The structural basis for the intrinsic disorder in the actin filament: The "lateral slipping" model, *J. Cell Biol.* **115,** 689–703.

Brown, J. H., Jardetzky, T. S., Gorga, J. C., Stern, L. J., Urban, R. G., Strominger, J. L., and Wiley, D. C. (1993) Three-dimensional structure of the human class II histocompatibility antigen HLA-DR1, *Nature* **364,** 33–39.

Brünger, A. T. (1992) X-PLOR Version 3.1: A system for X-ray crystallography and NMR, Yale Univ. Press, New Haven.

Carlier, M.-F., Didry, D., and Pantaloni, D. (1987) Microtubule elongation and guanosine 5′-triphosphate hydrolysis: Role of guanine nucleotides in microtubule dynamics, *Biochemistry* **26,** 4428–4437.

Carlier, M.-F., and Pantaloni, D. (1986) Direct evidence for ADP-Pi-F-actin as the major intermediate in ATP-actin polymerization: Rate of dissociation of Pi from actin filaments, *Biochemistry* **25,** 7789–7792.

Carlier, M.-F., Pantaloni, D., and Korn, E. D. (1984) Evidence for an ATP cap at the ends of actin filaments and its regulation of the F-actin steady state, *J. Biol. Chem.* **259,** 9983–9986.

Cedergren-Zeppezauer, E. S., Goonesekere, N. C. W., Rozycki, M. D., Myslik, J. C., Dauter, Z., Lindberg, U., and Schutt, C. E. (1994) Crystallization and structure determination of bovine profilin at 2.0 Å resolution, *J. Mol. Biol.* **240,** 459–475.

Chen, X., Cook, R. K., and Rubenstein, P. A. (1993) Yeast actin with a mutation in the "hydrophobic plug" between subdomains 3 and 4 ($L_{266}D$) displays a cold-sensitive polymerization defect, *J. Cell Biol.* **123,** 1185–1195.

Cho, Y., Gorina, S., Jeffrey, P. D., and Pavletich, N. P. (1994) Crystal structure of a p53 tumor suppressor-DNA complex: understanding tumorigenic mutations, *Science* **265,** 346–355.

DasGupta, G., and Reisler, E. (1992) Actomyosin interactions in the presence of ATP and the N-terminal segment of actin, *Biochemistry* **31,** 1836–1841.

DeRosier, D. J. (1990) The changing shape of actin, *Nature* **347,** 21–22..

Drechsel, D. N., and Kirschner, M. W. (1994) The minimum GTP cap required to stabilize microtubules, *Curr. Biol.* **4,** 1053–1061.

Egelman, E. H. (1994) The ghost of ribbons past, *Curr. Biol.* **4,** 79–81.

Engh, R. A., and Huber, R. (1991) Accurate bond and angle parameters for X-ray protein structure refinement, *Acta Crystallogr. A* **47,** 392–400.

Finkel, T., Theriot, J. A., Dise, K. R., Tomaselli, G. F., and Goldschmidt-Clermont, P. J. (1994) Dynamic actin structures stabilized by profilin, *Proc. Natl. Acad. Sci. USA* **91,** 1510–1514.

Frado, L.-L., and Craig, R. (1992) Electron microscopy of the actin-myosin head complex in the presence of ATP, *J. Mol. Biol.* **223,** 391–397.

Harrison, S. C., Olson, A. J., Schutt, C. E., Winkler, F. K., and Bricogne, G. (1978) Tomato bushy stunt virus at 2.9 Å resolution, *Nature* **276,** 368–373.

Hegyi, G., Michel, H., Shabanowitz, J., Hunt, D. F., Chatterjie, N., Healy-Louie, G., and Elzinga, M. (1992) Gln-41 is intermolecularly cross-linked to Lys-113 in F-actin by *N*-(4-azidobenzoyl)-putrescine, *Protein Sci.* **1,** 132–144.

Holmes, K. C. (1994) Solving the structures of macromolecular complexes, *Structure* **2,** 589–593.

Holmes, K. C., Popp, D., Gebhard, W., and Kabsch, W. (1990) Atomic model of the actin filament, *Nature* **347,** 44–49.

Huxley, H. E. (1963) Electron microscope studies on the structure of natural and synthetic protein filaments from striated muscle, *J. Mol. Biol.* **7,** 281–308.

Huxley, H. E. (1973) Structural changes in the actin and myosin containing filaments during muscle contraction, *Cold Spring Harbor Symp. Quant. Biol.* **37,** 361–376.

Hyman, A. A., Chrétien, D., Arnal, I., and Wade, R. H. (1995) Structural changes accompanying GTP hydrolysis in microtubules: Information from a slowly hydrolyzable analogue guanylyl-($\alpha,\beta$)-methylene-diphosphonate, *J. Cell Biol.* **128,** 117–125.

Kabsch, W., Mannherz, H.-G., Suck, D., Pai, E. F., and Holmes, K. C. (1990) Atomic structure of the actin:DNase I complex, *Nature* **347,** 37–44.

Korn, E. D., Carlier, M.-F., and Pantaloni, D. (1987) Actin polymerization and ATP hydrolysis, *Science* **238,** 638–644.

Kraulis, P. (1991) MOLSCRIPT: A program to produce both detailed and schematic plots of protein structures, *J. Appl. Crystallogr.* **24,** 946–950.

Lee, B., and Richards, F. M. (1971) The interpretation of protein structures: Estimation of static accessibility, *J. Mol. Biol.* **55,** 379–400.

Lepault, J., Ranck, J.-L., Erk, I., and Carlier, M.-F. (1994) Small angle X-ray scattering and electron cryomicroscopy study of actin filaments: Role of the bound nucleotide in the structure of F-actin, *J. Struct. Biol.* **112,** 79–91.

Lorenz, M., Popp, D., and Holmes, K. C. (1993) Refinement of the F-actin model against X-ray fiber diffraction data by the use of a directed mutation algorithm, *J. Mol. Biol.* **234,** 826–836.

Makowski, L. (1991) An estimate of the number of structural parameters measurable from a fiber diffraction pattern, *Acta Crystallogr. A* **47,** 562–567.

Mandelkow, E.-M., Mandelkow, E., and Milligan, R. A. (1991) Microtubule dynamics and microtubule caps: A time-resolved cryo-electron microscopy study, *J. Cell Biol.* **114,** 977–992.

McLaughlin, P. J., Gooch, J. T., Mannherz, H.-G., and Weeds, A. G. (1993) Structure of gelsolin segment 1-actin complex and the mechanism of filament severing, *Nature* **364,** 685–692.

Mendelson, R. A., and Morris, E. (1994) The structure of F-actin: Results of global searches using data from electron microscopy and X-ray crystallography, *J. Mol. Biol.* **240,** 138–154.

Milligan, R. A., Whittaker, M., and Safer, D. (1990) Molecular structure of F-actin and location of surface binding sites, *Nature* **348,** 217–221.

Mitchison, T., and Kirschner, M. (1984) Dynamic instability of microtubule growth, *Nature* **312,** 237–242.

Moens, P. D. J., Yee, D. J., and dos Remedios, C. G. (1994) Determination of the radial coordinate of Cys-374 in F-actin using fluorescence resonance energy transfer spectroscopy: Effect of phalloidin on polymer assembly, *Biochemistry* **33,** 13102–13108.

Namba, K., and Stubbs, G. (1986) Structure of tobacco mosaic virus at 3.6 Å resolution: Implications for assembly, *Science* **231,** 1401–1406.

Oosawa, F. (1977) Actin-actin bond strength and the conformational change of F-actin, *Biorheology* **14,** 11–19.

Orlova, A., and Egelman, E. H. (1992) Structural basis for the destabilization of F-actin by phosphate release following ATP hydrolysis, *J. Mol. Biol.* **227,** 1043–1053.

Orlova, A., and Egelman, E. H. (1993) A conformational change in the actin subunit can change the flexibility of the actin filament, *J. Mol. Biol.* **232,** 334–341.

Orlova, A., Yu, X., and Egelman, E. H. (1994) Three-dimensional reconstruction of a co-complex of F-actin with antibody Fab fragments to actin's $NH_2$ terminus, *Biophys. J.* **66,** 276–285.

Owen, C., and DeRosier, D. (1993) A 13 Å map of the actin-scruin filament from the *Limulus* acrosomal process, *J. Cell. Biol.* **123,** 337–344.

Pantaloni, D., and Carlier, M.-F. (1993) How profilin promotes actin filament assembly in the presence of thymosion $\beta_4$, *Cell* **75,** 1007–1014.

Pollard, T. D., Bhandari, D., MAupin, P., Wachstock, D., Weeds, A., and Zol, H. (1993) Direct visualization by electron microscopy of the weakly bound intermediates in the actomyosin ATPase cycle, *Biophys. J.* **64,** 454–471.

Pollard, T. D., and Cooper, J. A. (1986) Actin and actin-binding proteins. A critical evaluation of mechanisms and functions, *Annu. Rev. Biochem.* **55,** 987–1035.

Pring, M., Weber, A., and Bubb, M. R. (1992) Profilin–actin complexes elongate actin filaments at the barbed end, *Biochemistry* **31,** 1827–1836.

Rayment, I., Rypniewski, W. R., Schmidt-Bäse, K., Smith, R., Tomchick, D. R., Benning, M. M., Winkelmann, D. A., Wesenberg, G., and Holden, H. M. (1993a) Three-dimensional structure of myosin subfragment-1: A molecular motor, *Science* **261,** 50–58.

Rayment, I., Holden, H. M., Whittaker, M., Yohn, C. B., Lorenz, M., Holmes, K. C., and Milligan, R. A. (1993b) Structure of the actin–myosin complex and its implications for muscle contraction, *Science* **261,** 58–65.

Rozycki, M. D., Myslik, J. C., Schutt, C. E., and Lindberg, U. (1994) Structural aspects of actin-binding proteins, *Curr. Opin. Cell Biol.* **6,** 87–95.

Rozycki, M. D., Chik, J. K., Lindberg, U., and Schutt, C. E. (1995) Crystallographically observed conformational changes and sulfhydryl reactivity in actin, *Biophys. J.* **68,** 367s.

Schmid, M. F., Agris, J. M., Jakana, J., Matsudaira, P., and Chiu, W. (1994) Three-dimensional structure of a single filament in the *Limulus* acrosomal bundle: Scruin binds to homologous helix-loop-beta motifs in actin, *J. Cell Biol.* **124,** 341–350.

Schröder, R. R., Manstein, D. J., Jahn, W., Holden, H., Rayment, I., Holmes, K. C., and Spudich, J. A. (1993) Three-dimensional atomic model of F-actin decorated with *Dictyostelium* myosin S1, *Nature* **364,** 171–174.

Schutt, C. E. (1987) Movement on the *Aufbaubahn, Nature* **325,** 757–758.

Schutt, C. E., Lindberg, U., Myslik, J., and Strauss, N. (1989) Molecular packing in profilin-actin crystals and its implications, *J. Mol. Biol.* **209,** 735–746.

Schutt, C. E., and Lindberg, U. (1992) Actin as the generator of tension during muscle contraction, *Proc. Natl. Acad. Sci. USA* **89,** 319–323.

Schutt, C. E., and Lindberg, U. (1993) A new perspective on muscle contraction, *FEBS Lett.* **325,** 59–62.

Schutt, C. E., Myslik, J. C. Rozycki, M. D., Goonesekere, N. C. W., and Lindberg, U. (1993) The structure of crystalline profilin:β-Actin, *Nature* **365,** 810–816.

Schutt, C. E., Rozycki, M. D., and Lindberg, U. (1994) What's the matter with the ribbon? Curr. Biol. **4,** 185–186.

Schutt, C. E., Rozycki, M. D., Chik, J. K., and Lindberg, U. (1995) Structural studies on the ribbon-to-helix transition in profilin:actin crystals, *Biophys. J.* **68,** 12s–18s.

Shapiro, L., Fannon, A. M., Kwong, P. D., Thompson, A., Lehmann, M. S., Grübel, G., Legrand, J.-F., Als-Nielsen, J., Colman, D. R., and Hendrickson, N. A. (1995) Structural basis of cell–cell adhesion by cadherins, *Nature* **374,** 327–337.

Story, R. M., Weber, I. T., and Steitz, T. A. (1992) The structure of the *E. coli recA* protein monomer and polymer, *Nature* **355,** 318–325.

Sutoh, K. (1982) Identification of myosin-binding sites on the actin sequence, *Biochemistry* **22,** 1579–1585.

Tirion, M. M., ben-Avraham, D., Lorenz, M., and Holmes, K. C. (1995) Normal modes as refinement parameters for the F-actin model, *Biophys. J.* **68,** 5–12.

Vale, R. D., Coppin, C. M., Malik, F., Kull, F. J., and Milligan, R. A. (1994) Tubulin GTP hydrolysis influences the structure, mechanical properties, and kinesin-driven transport of microtubules, *J. Biol. Chem.* **269,** 23769–23775.